IMPACT OF ACTUAL INTERFERENCE ON CAPACITY AND CALL ADMISSION CONTROL IN A CDMA NETWORK

Asad Parvez, B.S.

Thesis Prepared for the Degree of

MASTER OF SCIENCE

UNIVERSITY OF NORTH TEXAS

May 2004

APPROVED:

Robert Akl, Major Professor
Robert Brazile, Committee Member and Graduate Coordinator
Steve Tate, Committee Member
Krishna Kavi, Chair of the Department of Computer Sciences
Oscar N. Garcia, Dean of the College of Engineering
Sandra L. Terrell, Interim Dean of the Robert B. Toulouse School of Graduate Studies

Parvez, Asad, Impact of actual interference on capacity and call admission control in a CDMA network. Master of Science (Computer Science), May 2004, 57 pp., 2 tables, 41 figures, 42 titles.

An overwhelming number of models in the literature use average inter-cell interference for the calculation of capacity of a Code Division Multiple Access (CDMA) network. The advantage gained in terms of simplicity by using such models comes at the cost of rendering the exact location of a user within a cell irrelevant. We calculate the actual per-user interference and analyze the effect of user-distribution within a cell on the capacity of a CDMA network. We show that even though the capacity obtained using average interference is a good approximation to the capacity calculated using actual interference for a uniform user distribution, the deviation can be tremendously large for non-uniform user distributions.

Call admission control (CAC) algorithms are responsible for efficient management of a network's resources while guaranteeing the quality of service and grade of service, i.e., accepting the maximum number of calls without affecting the quality of service of calls already present in the network. We design and implement global and local CAC algorithms, and through simulations compare their network throughput and blocking probabilities for varying mobility scenarios. We show that even though our global CAC is better at resource management, the lack of substantial gain in network throughput and exponential increase in complexity makes our optimized local CAC algorithm a much better choice for a given traffic distribution profile.

ACKNOWLEDGMENTS

First and foremost, I would like to thank my advisor Dr. Robert Akl for taking on multitudes of roles that provided direction from the inception to the conclusion of this work. His unfaltering patience, relentless meticulosity, and astonishing enthusiasm has not only been invaluable but has also left an indelible mark on me. I am highly indebted to the members of my committee Dr. Robert Brazile and Dr. Steve Tate for their careful reading and suggestions.

I extend my gratitude to Jackie Stanczyk and my colleagues at SCS computing center for providing humor when it was needed the most. I am also very grateful to my parents for their love and many years of support. Above all, I would like to thank Chiang, Hui-Yi who has been an inspiration and a partner in this journey we started a year ago.

CONTENTS

LIST OF TABLES

LIST OF FIGURES

CHAPTER 1

INTRODUCTION

Wireless communication is now one of the largest and the fastest growing segments of the telecommunication market. The tremendous growth in commercial wireless systems is an indication that the reliability, affordability, and the quality of these services, complemented by inherent convenience is rivaling conventional systems. Economics of scale has driven down the cost of wireless equipment within the affordable range for a large percentage of the population. The ubiquitous mobile phones and disappearing land lines are the harbinger of a truly wireless world. The dazzling array of much more capable and versatile mobiles available today provides glimpses into such a world. The immense possibilities and increasing user demand are propelling the growth of such wireless technologies.

Code Division Multiple Access (CDMA) is one such technology created to meet the increasing demands and to overcome the obstacles plaguing existing wireless systems. The ability to offer greater capacity and multi-rate transmission, seamless integration, and easier migration path to 3G cellular systems has fueled the widespread deployment of CDMA systems all over the world. But the principal attraction has always been the ability to carry higher capacity than Time Division Multiple Access (TDMA) and Frequency Division Multiple Access (FDMA) systems, which explains multitudes of research devoted to study capacity of CDMA systems.

1.1 CDMA Overview

CDMA is a relatively new wireless access technology introduced by Qualcomm in early 90's. It follows a different approach from existing technologies such as TDMA and FDMA, which

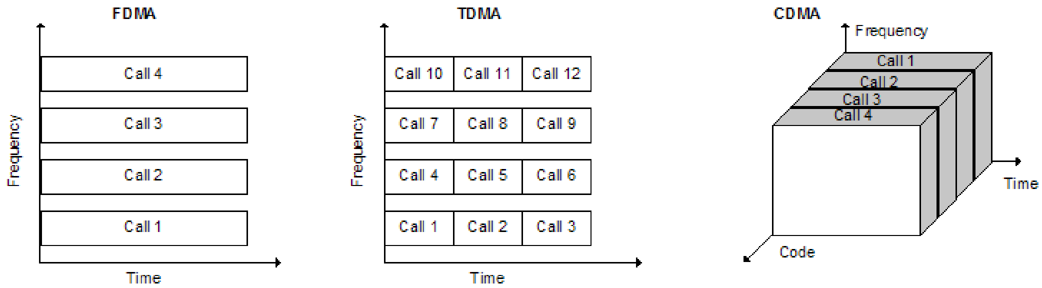

Figure 1.1: Comparison between FDMA, TDMA, and CDMA.

accommodates calls in different time slots, and frequency subbands, respectively. Instead of sharing available bandwidth in either time or frequency, it lets all the users occupy the whole allocated bandwidth at the same time. The distinction between calls is made possible by assigning unique codes to each call. Fig. 1.1 shows the functional difference between these three prevalent multiple access technologies.

CDMA has been shown to have many advantages over TDMA and FDMA in network capacity, immunity to multi-path fading, voice activity and handoff mechanism [25, 36]. CDMA is based on spread spectrum communication [13, 35], a technique originally developed during World War II. Originally, the idea of spread spectrum was to spread the signal over a large number of narrowband channels by hopping the signal over these channels in a pseudo-random fashion. This spreading technique is known as Frequency Hopping (FH). Later, another spreading technique was developed, called Direct Sequence (DS), which modulates the data with a fast pseudo-random code sequence. Today, DS is the prominent choice among spreading techniques, and is the only one considered in this work.

When using DS-CDMA, different codes are assigned to different users. These codes are used to spread and despread the users' messages. The codes for other users are assigned in such a way they produce very small signal levels when a signal is being despread, but produce a much higher signal level for the code associated with the intended user. Consequently, the other signals are rejected as noise. However, as the number of users increases, the signal levels also increase, and at some point with increasing users, it is no longer possible to distinguish between noise and a user's signal. The capacity of a CDMA network is therefore limited by the amount of interference that can be tolerated from other users. And since CDMA capacity is limited by interference [12, 30, 39], it is inevitable to investigate the factors involved in determining interference.

The study of capacity characteristics for a CDMA network has been the subject of extensive research. Power control, voice activity factor, and soft handoff are a few of the techniques employed to reduce interference. Since the capacity is interference bound, which in turn is dependant on power control, a large percentage of effort has been invested in developing better power control algorithms [7, 11, 14, 15, 28, 33, 40]. Most of these algorithms try to solve the near-far-problem, i.e., the power received from a mobile near its base station is much more than the power received from a mobile at the boundary of that cell. Interference can also be reduced by using voice activity detection, which reduces the rate of the speech coder when silent periods are detected in the speech waveform. Soft handoff of calls is one of the biggest attractions of CDMA. It enables a smoother transition of a moving call from one cell to another, unlike TDMA and FDMA where a connection is broken, and then established again. Soft handoff's contribution in increasing capacity for a heavily loaded CDMA network is quite significant [36].

Another issue is whether CDMA capacity is bounded by reverse link capacity or forward link capacity. In [5, 8, 16, 25, 27, 29, 31, 32, 36, 37], the authors have concluded that reverse link capacity is lower than forward link capacity. In this work, we consider the reverse link capacity only.

Most of the models used for capacity analysis use average inter-cell interference instead of actual inter-cell interference [22, 4, 34, 18]. Thus, the inter-cell interference caused by different users in the same cell is the same, and is independent of their exact location within the cell.

Due to dependence of capacity on interference, call admission control (CAC) algorithm design is crucial in guaranteeing quality of service and grade of service provided by the network. There are two approaches that most CAC algorithm design fall under - global and local. A global CAC algorithm decision to admit a call in a cell is based on the number of calls in all the cells in the network. On the other hand, a local CAC algorithm decision to admit a call in a cell is based on the number of calls already admitted in that cell only.

1.2 Objectives

In this work, we investigate the effect of using actual interference instead of average interference on the network capacity and call admission control mechanism for a CDMA network through computer simulations. For comparison, we are using the network described in [2] that uses average interference in the calculation of the capacity and call admission control. The simulator designed is an extension to the software tools CCAP (CDMA Capacity Allocation and Planning) [1].

The objectives of this work are as follows:

- **Capacity Analysis:**
  - Formulation of inter-cell interference model using exact location of users in a cell.
  - Comparison of network capacity obtained using actual interference with capacity obtained using average interference.
- **Call Admission Control:**
  - Development of global and local call admission control algorithms.
  - Comparison of network throughput and blocking probabilities for the global CAC using actual and average interference.
  - Comparison of global and local CAC performance in terms of blocking probabilities and network throughput for different traffic distribution profiles.

1.3 Organization

In Chapter 2, we investigate the effect of using exact location of users for calculation of inter-cell interference when calculating the capacity of a CDMA network. We compare the network capacity obtained using actual interference with capacity obtained using average interference.

In Chapter 3, we design a global CAC algorithm. We measure the network performance in terms of blocking probabilities and network throughput for average and actual interference.

In Chapter 4, we design a local CAC algorithm. We compare the performance of our local CAC algorithm with a traditional CAC algorithm where the maximum number of calls admitted is the same for every cell.

In Chapter 5, we compare the performance of our global and local CAC algorithms in terms of blocking probabilities and network throughput for non-uniform traffic distribution profiles.

Finally, in Chapter 6, we present our conclusions and summarize the contributions of this work.

CHAPTER 2

INTERFERENCE MODEL IMPACT ON CAPACITY

2.1 Introduction

Since CDMA capacity is limited by interference [12, 30, 39], it is inevitable to investigate the factors involved in determining interference. One of such variables is the user's distance from base stations. It has been shown in [5, 8, 16, 25, 27, 29, 31, 32, 36, 37] that the capacity of a CDMA network is reverse link limited, and hence our study is confined to reverse link capacity. One of the principal characteristics of a CDMA network is that the capacity of the system is a function of total interference experienced by the network, and is upper bounded by the cell experiencing the most interference. Thus, it is imminent to characterize total inter-cell interference seen by a single cell in terms of the user distribution in every other cell for determining capacity in that single cell.

Traditionally, the total interference contributed by a cell has been viewed as an approximation, determined by simply multiplying the number of users in that cell by the average interference offered by that cell [12]. In other words, a user placed anywhere within a cell generated the same amount of inter-cell interference. Clearly, a more realistic approach will use per-user interference as a function of their actual distance to the point of interest. There is a dearth of literature where actual distance was used in the interference model. In [22], even though interference was calculated using actual distance, the capacity calculations were done using mean value of interference. User positions were varied over time, but the number of users was kept constant. In [17], authors quantify the cell capacity by focusing on location of active users but they categorize the location of users in two zones - near and far. Also, their network model comprises of only three cells.

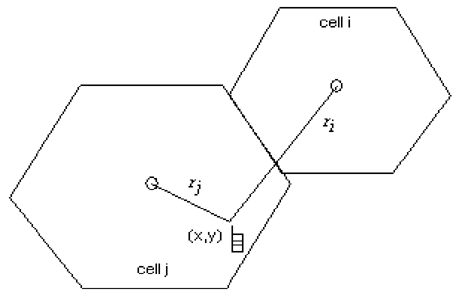

Figure 2.1: Inter-cell interference on cell i from users in cell j.

We use a model where interference is calculated with actual distance to investigate the effect of user distribution on reverse link capacity. Computer simulations of a CDMA network are carried out where interference is calculated in real time as the network is being populated. We assume several user distributions. We investigate the cases of equal capacity in every cell as well as the capacity obtained through optimization techniques discussed in [2]. We verify the numerical analysis results published in [2], and also show that it is possible to have much higher or lower capacity if actual interference is used for specific user distributions.

2.2 Relative Average Inter-Cell Interference Model

Consider two cells i and j. The user is power controlled by the base station of cell j, and is at distance $r_j(x, y)$ from the base station. The distance of the same user from the base station in cell i is $r_i(x, y)$ as shown in Fig. 2.1. Let n_j be the number of users in cell j, denoted by region C_j and area A_j=Area(C_j). The user's transmitter power gain equals the propagation loss in cell j. The propagation loss is generally modeled as the product of the mth power of distance and a log-normal component representing shadowing losses. The large scale path loss and shadow fading are assumed to be circumvented by the power control mechanism. However, it cannot compensate for the fast fluctuations of the signal power associated with Rayleigh fading [12]. Let χ_i denote the Rayleigh random variable that represents the fading on the path from this user to cell i. Then, the relative average interference at cell i caused by n_j users in cell j is given by [2]

$$I_{ji} = \mathrm{E}\left[\iint\limits_{C_j} \frac{r_j^m(x,y)10^{\zeta_j/10}}{r_i^m(x,y)/\chi_i^2} \; \frac{n_j}{A_j} \; dA(x,y)\right], \tag{2.1}$$

where ζ is the decibel attenuation due to shadowing, with zero mean and standard deviation σ_s. This reduces to

$$I_{ji} = e^{(\gamma\sigma_s)^2} \; \frac{n_j}{A_j} \; \iint\limits_{C_j} \frac{r_j^m(x,y)}{r_i^m(x,y)} \; dA(x,y), \tag{2.2}$$

where $\gamma = \ln(10)/10$. (2.2) is used to calculate the relative average inter-cell interference for a uniform user distribution. To obtain the per-user inter-cell interference, F_{ji}, I_{ji} is divided by the total number of users in cell j. Note that in this model, F_{ii} equals zero. F_{ji} can be viewed as elements in a two dimensional matrix F with $i, j = 1, ..., M$, where M is the total number of cells in the network. Each column i of F contains the per-user inter-cell interference exerted by cell j on every other cell i. Consequently, the total relative average inter-cell interference experienced by cell i is simply the summation of the product of number of users n_j in cell j and their respective per-user interference factor F_{ji}, which is the column vector i in F,

$$I_i = \sum_{j=1}^{M} n_j F\left[j, i\right]. \tag{2.3}$$

Once matrix F is computed in advance, the above calculation is adequately fast since it requires only M lookups in the matrix. However, the interference caused by a user is independent of its location within a given cell.

2.3 Relative Actual Inter-Cell Interference Model

If the user's exact location within a cell is taken into account for determining its interference to the network, the matrix F cannot be used. Instead, a new matrix U is computed as follows. For a user k in cell j, the relative actual interference offered by this user to cell i is

$$(U_{ji})_k = e^{(\gamma\sigma_s)^2} \left(\frac{r_j}{r_i}\right)^m . \tag{2.4}$$

Hence, the total relative actual inter-cell interference at cell i caused by every user in the network is

$$I_i = \sum_{j=1}^{M} \sum_{k=1}^{n_j} (U_{ji})_k \, , \text{for} \quad i \neq j. \tag{2.5}$$

The calculation of the interference is now much more time consuming since the matrix U has to be updated every time a user enters the network. However, instead of relative average interference values, it stores the actual interference caused by each user on every cell.

2.4 Capacity

The capacity of a CDMA network is determined by maintaining a lower bound on the bit energy to interference density ratio which is given by [9]

$$\left(\frac{E_b}{I_0}\right)_i = \frac{E_b}{\alpha(RE_b)\left(n_i - 1 + I_i\right)/W + N_0}, \quad \text{for} \quad i = 1, ..., M, \tag{2.6}$$

where the network has a spread signal bandwidth of W, information rate of R bits/sec, voice activity factor of α, background noise spectral density of N_o, and n_i users in cell i. To achieve the required bit error rate $\left(\frac{E_b}{I_0}\right)_i$ must be maintained above a certain threshold. If τ denotes that threshold, then by rewriting the above equations, we get an upper bound on the number of users in every cell i:

$$n_i + I_i \leq \frac{W/R}{\alpha}\left(\frac{1}{\Gamma} - \frac{1}{E_b/N_0}\right) + 1 \triangleq c_{eff}, \quad \text{for} \quad i = 1, ..., M. \tag{2.7}$$

A feasible user configuration of the network is a set of users in their respective cells that satisfies the above equations. In other words, a new user is admitted to the network if its admittance still maintains the above inequalities for every cell. The right hand side of the equations is a constant that depends on the system parameters, and essentially determines the effective number of channels available to the network.

2.4.1 Equal Capacity

Equal capacity is defined as the requirement that all cells have an equal number of users, i.e., n_i = n for all i.

2.4.2 Optimized Capacity

The optimized network capacity is the solution to the following optimization problem:

$$\begin{aligned} \max_{\underline{n}} \quad & \sum_{i=1}^{M} n_i, \\ \text{subject to} \quad & n_i + I_i \leq c_{eff}, \\ & \text{for} \quad i = 1, ..., M. \end{aligned} \tag{2.8}$$

In [2], the authors describe a technique to solve this Integer Programming (IP) optimization problem. By assuming integer variables n_i, $i = 1, ..., M$ to be continuous variables the IP problem (2.8) becomes a Linear Programming (LP) problem whose solution can be obtained by any general LP technique, e.g., the simplex method [6].

2.5 Numerical Results

The simulator designed for comparison of the two interference models is an extension to the software tools CCAP (CDMA Capacity Allocation and Planning) [1]. CCAP, written in MATLAB, was developed at Washington University in St. Louis for numerical analysis of optimization techniques developed in [2] to determine and maximize the capacity of CDMA networks. The analysis in CCAP was carried out with relative average interference. Our simulator can verify the numerical analysis results produced by CCAP and also use the actual distance of users for calculation of exact interference. It has the capability to populate, remove, and relocate users within the network.

The testbed is an exact configuration of the network model used in [2]. The COST-231 propagation model with a carrier frequency of 1800 MHz, average base station height of 30 meters and average mobile height of 1.5 meters is used to determine the coverage region. The path loss coefficient, m, is 4. The shadow fading standard deviation, σ_s, is 6 dB. The processing gain, $\frac{W}{R}$, is 21.1 dB. The bit energy to interference ratio threshold, Γ, is 9.2 dB. The interference to background noise ratio, $\frac{I_0}{N_0}$, is 10 dB. The voice activity factor, α, is 0.375. These parameters give c_{eff} of 38.25, which is the implicit upper bound on the relative interference in every cell.

We analyze a twenty-seven cell CDMA network with uniform user distribution. We compared the capacity calculated with relative average interference as well as relative actual interference. For the equal capacity case, the network capacity is 486 with 18 users per cell if average interference is used. The capacity in each cell is given in parentheses and the total relative average inter-cell interference is given in brackets as shown in Fig. 2.2. Using the actual distance for interference calculation always results in 17 users per cell as shown in Fig. 2.3.

The optimization in (2.8) results in a network capacity of 559 users when using average interference as shown in Fig. 2.4. Using the actual relative interference, a simulation is run for several hundred trials. Figures 2.5, 2.6, and 2.7 show three of those trials, with network capacity of 554, 564, and 568 respectively. The values are found to be adequately close to those in Fig. 2.4. Fig. 2.8 shows the cell capacity for those three trials and for the average interference case. Furthermore, fifty simulation trials reveal the average of each cell capacity converging towards the optimized values obtained numerically, as shown in Fig. 2.9.

The user distribution is uniform for all the above cases. However, for non-uniform user distribution in the cells, our simulation results show the extreme diversity in the capacity of

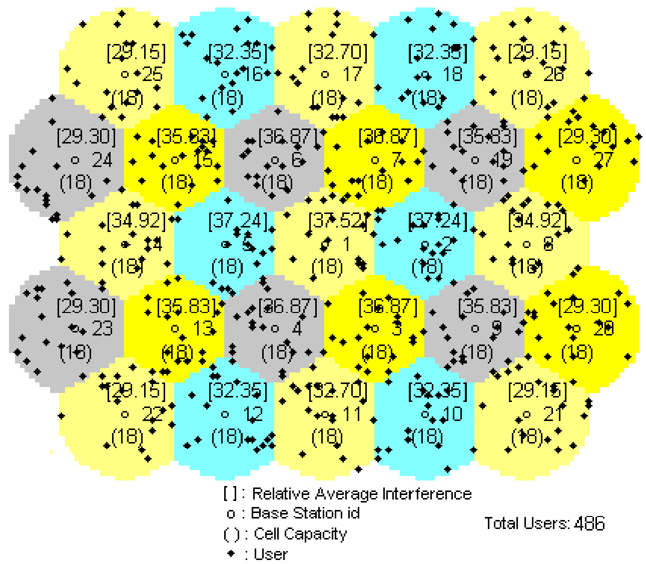

Figure 2.2: Equal capacity with uniform user distribution using average interference.

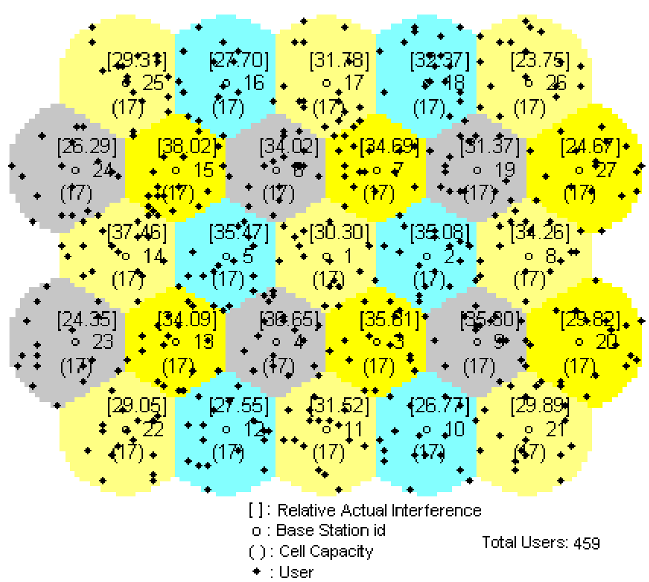

Figure 2.3: Equal capacity with uniform user distribution using actual interference.

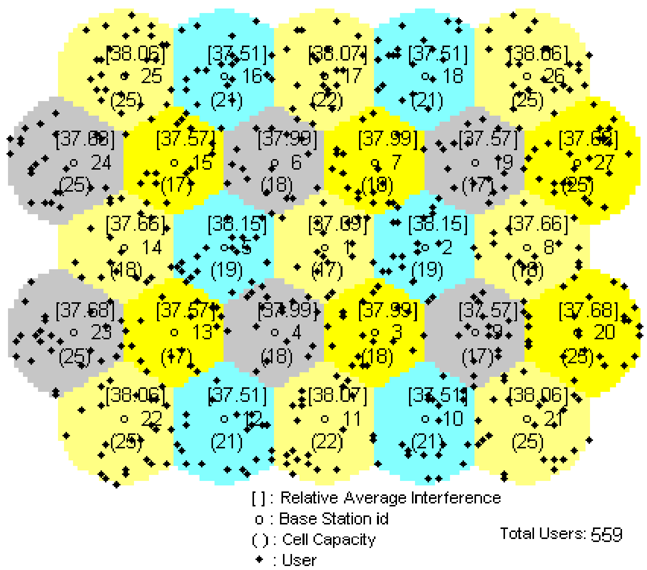

Figure 2.4: Optimized network capacity of 559 using average interference.

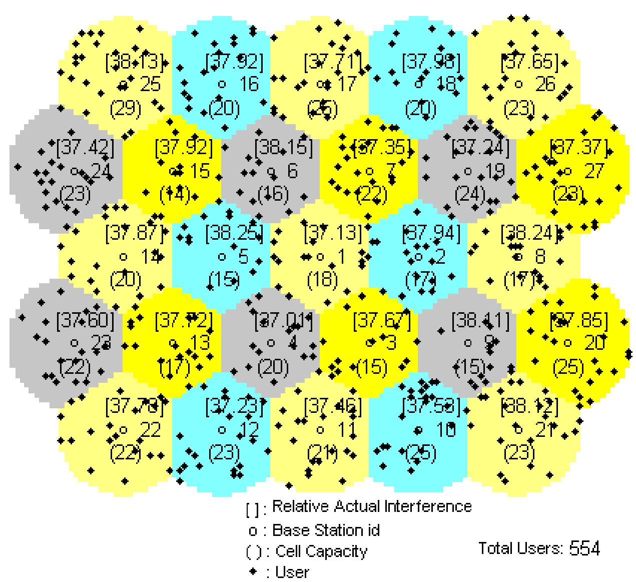

Figure 2.5: Simulated network capacity of 554 using actual interference.

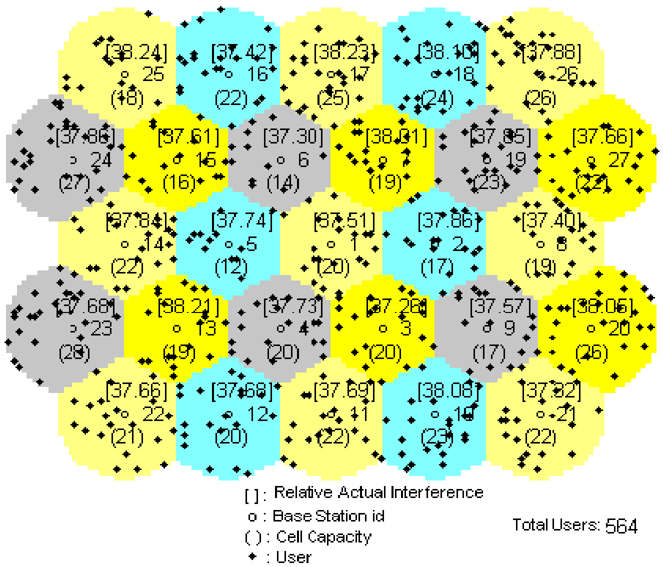

Figure 2.6: Simulated network capacity of 564 using actual interference.

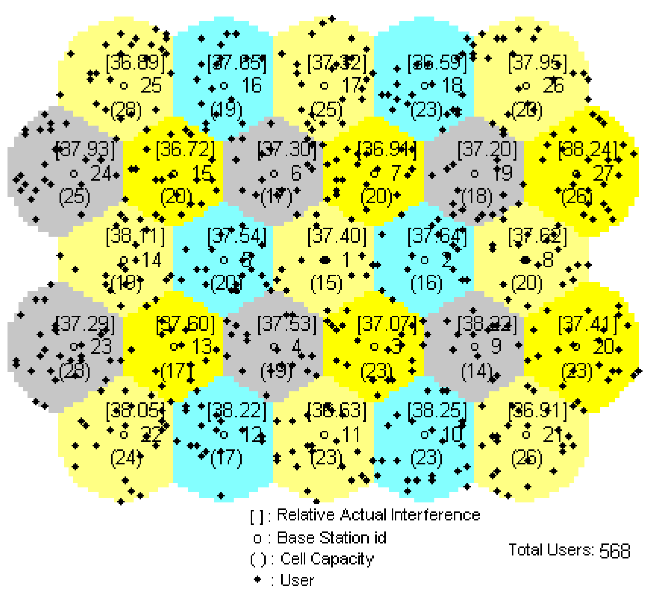

Figure 2.7: Simulated network capacity of 568 using actual interference.

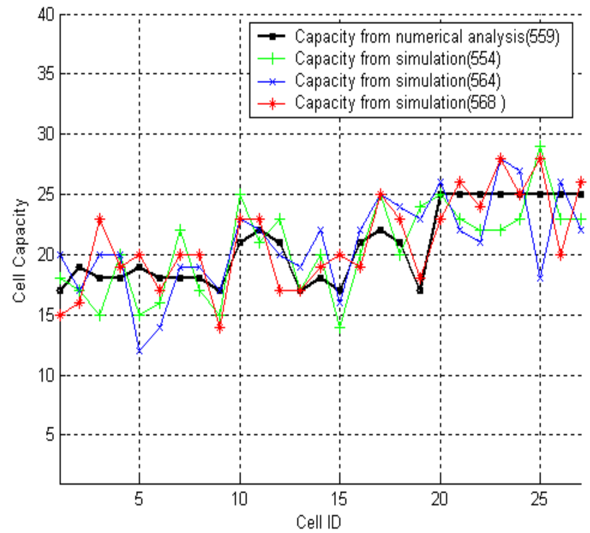

Figure 2.8: Comparison of cell capacity for 3 simulation trials, with optimized capacity obtained numerically.

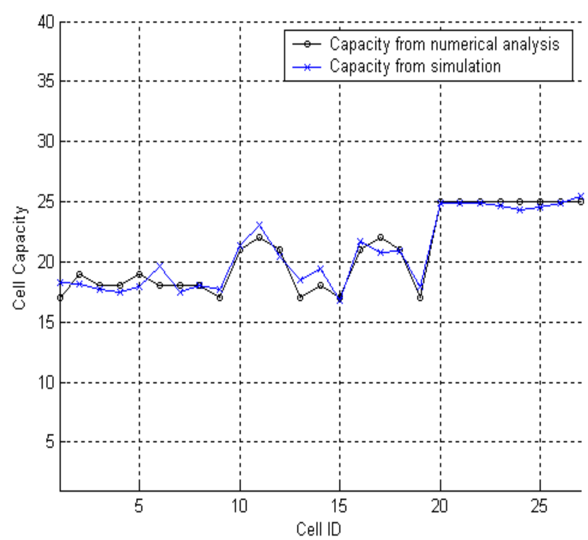

Figure 2.9: Comparison of average cell capacity for 50 simulation trials, with optimized capacity obtained numerically.

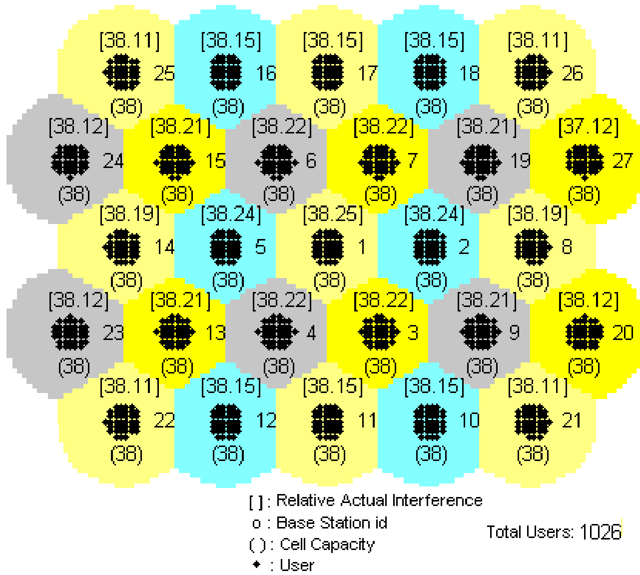

Figure 2.10: Maximum network capacity of 1026 using actual interference with best case non-uniform user distribution scenario.

the network. Changing the placement of the users in such a way that they cause minimum interference to the whole network, instead of placing them randomly in their cells, yields a much higher capacity of 1026 users with 38 users in each cell. Fig. 2.10 shows the pattern in which users were placed. The high concentration of users near their respective base station is justified, since intuitively, the obvious way to have minimum inter-cell interference on the network is to remain closer to one's base station, reducing the power gain required to maintain a desired signal to noise ratio.

On the other hand, the maximum network capacity is very low if the simulator places the users in such a way that they cause maximum interference to the network. The simulation yielded a total capacity of 108 users, with only 4 users in each cell. The pattern seen in Fig. 2.11 shows that the simulator placed the users at the extreme corners of their respective cells. The placement at extremities would require users to increase their power gain causing a lot more interference to other users. It is interesting to see that cells 9, 13, 15, and 19 where interference peaked are not in the center of the network. This is justified since the users in the cells at the boundaries of the network are placed near the periphery of these

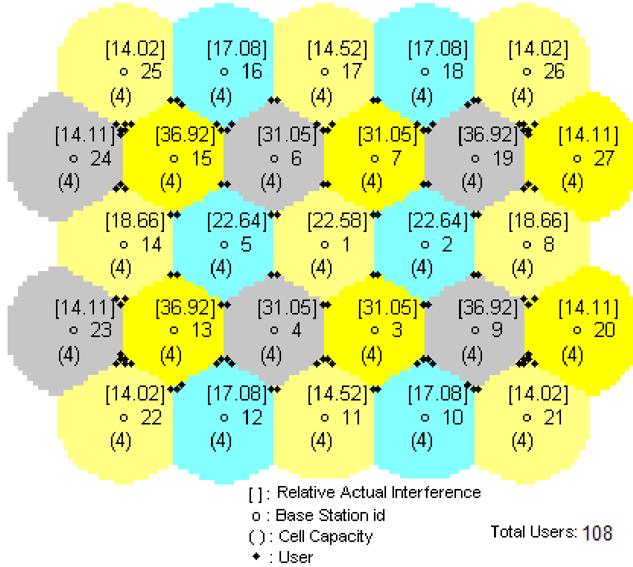

Figure 2.11: Maximum network capacity of 108 using actual interference with worst case non-uniform user distribution scenario.

cells, and towards the center of the network, resulting in much higher concentration of users along the boundaries of these 4 cells.

2.6 Summary

We investigate the effect of using the actual distance of users for calculation of inter-cell interference when calculating the capacity of a CDMA network. The simulations are carried out for a twenty-seven cell CDMA network. We first simulate and verify the results that were obtained analytically using the relative average interference. Our simulation results show that for a uniform user distribution, the difference in capacity determined using relative actual interference and relative average interference is too small to warrant the incursion of heavy computational load involved in the former case. However, our simulations also show the extreme variation in total capacity under certain user placements, which could not have been predicted using the average interference for non-uniform user distributions.

CHAPTER 3

GLOBAL CALL ADMISSION CONTROL

3.1 Introduction

An efficient use of available resources is crucial for a network to guarantee quality of service, i.e., quality of communication, and grade of service, i.e., the blocking rate. It is call admission control's (CAC) responsibility to protect a network from performance degradation. Due to dependence of network capacity on interference contributed by every call in every cell, the design of a CDMA network CAC algorithm is relatively harder than the design of a CAC algorithm for a TDMA or FDMA network. There are two approaches that most CAC algorithms design fall under - local and global. A local CAC algorithm considers only a single cell for making a call admittance decision even though its design may look at the network as a whole. A global CAC algorithm takes the entire network into account to make every call processing decision. It is quite obvious that the global call admission control is a daunting process and imposes severe penalties on time and resources required for making decisions. However, since it offers the best view of the network, it is worthwhile to investigate the implementation of such an algorithm.

Since our global CAC algorithm takes mobility into account, a mobility model needs to be formulated. There are several mobility models that have been discussed in the literature [10, 19, 21, 20, 23, 24, 38, 41]. The mobility model that our CAC algorithms implement are presented in [3] where a call stops occupying a cell because, either user mobility has forced the user to hand off the call to another cell, or because the call is completed.

3.2 Mobility Model

The call arrival process to cell i is assumed to be a Poisson process with rate λ_i independent of other call arrival processes. The call dwell time is a random variable with exponential distribution having mean $1/\mu$, and it is independent of earlier arrival times, call durations and elapsed times of other users. At the end of a dwell time a call may stay in the same cell, attempt a handoff to an adjacent cell, or leave the network. Let q_{ij} be the probability that a call in progress in cell i after completing its dwell time goes to cell j. If cells i and j are not adjacent, then $q_{ij} = 0$. Let q_{ii} be the probability that a call in progress in cell i remains in cell i after completing its dwell time. In this case a new dwell time that is independent of the previous dwell time begins immediately. We denote by q_i the probability of departure from the network of a call in progress in cell i. The advantage of this mobility model is that we can simulate different mobility scenarios by varying the values of these probability parameters. By keeping q_i constant, and varying q_{ii} and q_{ij}, we can have a constant call dwell time, irrespective of its origin, over varying mobility scenarios.

Let $\mathcal{A}_i$ be the set of cells adjacent to cell i. Let ν_{ji} be the handoff rate out of cell j offered to cell i. The handoff traffic from cell j to an adjacent cell i is the sum of the proportion of new calls accepted in cell j that go to cell i and the proportion of handoff calls accepted from cells adjacent to cell j that go to cell i. Thus

$$\nu_{ji} = \lambda_j(1 - B_j)q_{ji} + (1 - B_j)q_{ji} \sum_{x \in \mathcal{A}_j} \nu_{xj}, \tag{3.1}$$

where B_j is the new call blocking (or handoff call blocking) probability for cell j. (3.1) can be rewritten as

$$\nu_{ji} = (1 - B_j)\, q_{ji}\rho_j, \tag{3.2}$$

where ρ_j, the total offered traffic to cell j, is given by

$$\rho_j = \lambda_j + \sum_{x \in \mathcal{A}_j} \nu_{xj} = \lambda_j + \nu_j. \tag{3.3}$$

3.3 Global Call Admission Control Algorithm

The call admission requirements that must be met in order to guarantee the quality of service is that the total simultaneous calls must satisfy

$$C_i = n_i + I_i \leq c_{eff},$$
$$\text{for} \quad i = 1, ..., M. \tag{3.4}$$

A new call or a handoff call arriving in cell i is blocked if this call leads to a violation of any of the above inequalities, i.e., causing interference that no longer meets the $\left(\frac{E_b}{I_0}\right)$ constraints from (2.7).

3.4 Simulator Model

The simulator is constructed as a sequential state machine running in a loop, where every loop cycle corresponds to a single time unit. It consists of two modules that are executed in sequential order - call arrival and admission module, and call removal module as shown in Fig. 3.1. The call arrival control is responsible for cell selection and determining arrival rates for each cell. The call admission control, implements the global CAC algorithm by enforcing the conditions specified by (3.4). Finally, the call removal control relocates and removes users depending on the mobility parameters.

3.4.1 Call Arrival and Admission Module

The module is comprised of two parts, call arrival control and call admission control. First, call arrival control generates actual arrival rates for each cell as input to the network and computes the total offered traffic to each cell. The total offered traffic $\rho_i(t)$ to cell i for time unit t is calculated as

$$\rho_i(t) = \lambda_i(t) + \nu_i(t) \quad \text{for} \quad i = 1, ..., M, \tag{3.5}$$

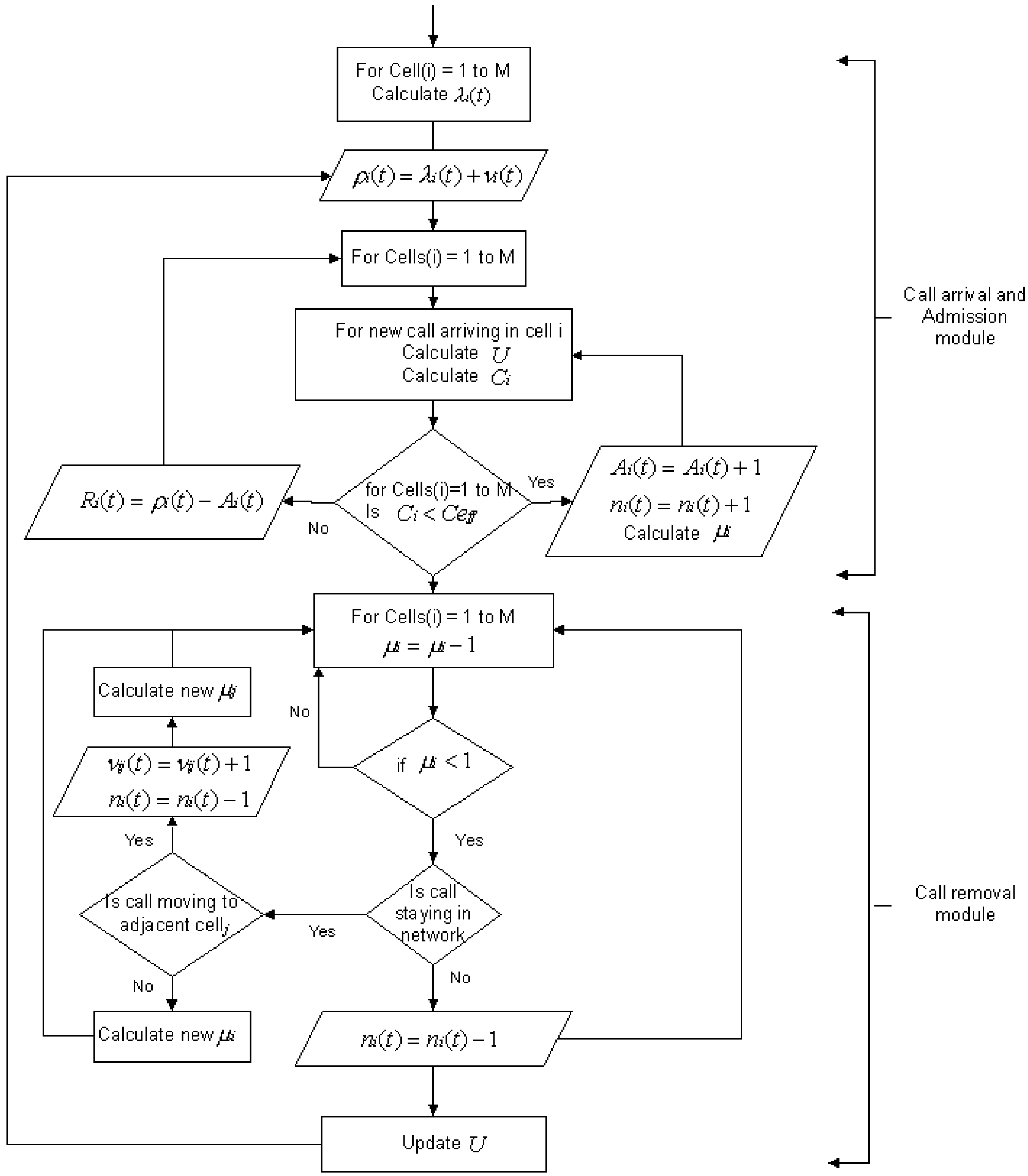

Figure 3.1: Flowchart of the network simulator for our global CAC algorithm.

where $\nu_i(t)$ are the calls that moved to cell i at time $t-1$. Note that $\nu_i(1)$=0, for $i = 1, ..., M$. The call arrival control then selects each call randomly for a randomly chosen cell, and passes it to call admission control along with the information about this new call.

In order to determine if the call can be admitted, call admission control computes C_i to check if the conditions given by (3.4) still hold if the call is allowed to enter the network.

Actual Interference

If the actual distance of the call k from its base station is being used to calculate interference, then the algorithm updates the interference matrix U, described in Chapter 2, in order to account for the increase in interference due to admitting the new call. It starts by constructing an array of relative interference caused by call k in cell i to all other cells j. From (2.4)

$$(U_{ij})_k = e^{(\gamma\sigma_s)^2} \left(\frac{r_i}{r_j}\right)^m \quad \text{for} \quad j = 1, ..., M. \tag{3.6}$$

And, row i of U, which contains the per-user inter-cell interference exerted by cell i on every other cell j is updated as

$$U[i,j] = U[i,j] + (U_{ij})_k \quad \text{for} \quad j = 1, ..., M. \tag{3.7}$$

Now, the new set of $C_i(t)$ is calculated as

$$C_i(t) = n_i(t) + \sum_{j=1}^{M} U[j,i] \quad \text{for} \quad i = 1, ..., M, \tag{3.8}$$

where $n_i(t)$ is the number of calls already present in cell i at time t.

Average Interference

If average interference is being used for calculation of capacity, then we already have the matrix F constructed in advance. In this case, the new set of $C_i(t)$ is calculated as

$$C_i(t) = n_i(t) + \sum_{j=1}^{M} n_j F[j,i] \quad \text{for} \quad i = 1, ..., M. \tag{3.9}$$

If the inequalities in (3.4) still hold for the new C_i's, then the call is allowed to enter the network, otherwise the call is rejected. Let $A_i(t)$ be the number of calls admitted in cell i during time period t. If the call is admitted, $A_i(t)$ and $n_i(t)$ are increased by one, its dwell time is calculated, and the control is passed back to the call arrival control. The cycle continues until all the arriving calls for this time unit have been processed. The number of rejected calls $R_i(t)$ for cell i during this time unit is calculated by subtracting $A_i(t)$ from the total offered traffic $\rho_i(t)$.

3.4.2 Call Removal Module

The module starts by reducing the dwell time of every call present in the network by one time unit. Then, for every call whose dwell time is less than one time unit, the following decision is made depending on the probability parameters: q_i, q_{ii}, and q_{ij}. The call can either leave the network, or stay in the network. If it is staying in the network, then it can either stay in the same cell with a new dwell time without being considered a new call, or it can move to one of its randomly selected adjacent cells. The handoff calls are considered as new calls, and are processed again through the call arrival and admission control module.

3.5 Network Throughput

The network throughput is defined as the number of calls per unit time that are admitted and stay in the network till termination without being dropped from the network. Since handoff calls are considered new admitted calls they are discounted from throughput calculation for time period t since they have already been accounted for in time unit $t-1$. Thus, the network throughput H_T over a time period T is given by

$$H_T = \frac{1}{T}\sum_{t=1}^{T}\left[\sum_{i=1}^{M}\left(A_i(t) - \nu_i(t)\right)\right]. \tag{3.10}$$

3.6 Blocking Probability

The blocking probability for a cell i is defined as the ratio of rejected calls to total offered traffic to that cell. The blocking probability for a cell i over a time period of T is given by

$$(B_T)_i = \frac{1}{T}\sum_{t=1}^{T}\left[\frac{R_i(t)}{\rho_i(t)}\right] \tag{3.11}$$

Intuitively, a lower blocking probability translates to a higher throughput.

3.7 Numerical Results

The network topology is the same as in Chapter 2. The traffic distribution is not uniform. This is modeled as two different call arrival rates. We choose the call arrival rates to be equal to 14 calls per unit time for all cells in Group A, i.e., (cells 5, 13, 14, and 23) and Group B, i.e., (cells 2, 8, 9, and 19). For the remaining cells, the call arrival rates are equal to 3 calls per unit time. Since all the parameters are the same as before, the upper bound c_{eff} for every cell in the network is still 38.25, which determines if an arriving call can be admitted.

Three mobility scenarios are considered: no mobility, low mobility, and high mobility of users. The probabilities for all cells i and j for the no mobility case are:

- q_{ij}, the probability that a call in cell i goes to cell $j = 0$.
- q_{ii}, the probability that a call in cell i stays in cell $i = 0.3$.
- q_i, the probability that a call in cell i leaves the network $= 0.7$.

The probability parameters for the low and high mobility cases are given in Tables 3.1 and 3.2 respectively.

As we can see from Figures 3.2, 3.3, and 3.4 that there is very little difference between maximum users admitted in all the cells for the network using average interference and

Table 3.1: The low mobility probabilities.

$\|\mathcal{A}_i\|$	q_{ij}	q_{ii}	q_i
3	0.020	0.240	0.700
4	0.015	0.240	0.700
5	0.012	0.240	0.700
6	0.010	0.240	0.700

- $\|\mathcal{A}_i\|$ is the number of cells adjacent to cell i.
- q_{ij} is the probability a call in cell i goes to cell j.
- q_{ii} is the probability a call in cell i stays in cell i.
- q_i is the probability a call in cell i leaves the network.

Table 3.2: The high mobility probabilities.

$\|\mathcal{A}_i\|$	q_{ij}	q_{ii}	q_i
3	0.100	0.000	0.700
4	0.075	0.000	0.700
5	0.060	0.000	0.700
6	0.050	0.000	0.700

- $\|\mathcal{A}_i\|$ is the number of cells adjacent to cell i.
- q_{ij} is the probability a call in cell i goes to cell j.
- q_{ii} is the probability a call in cell i stays in cell i.
- q_i is the probability a call in cell i leaves the network.

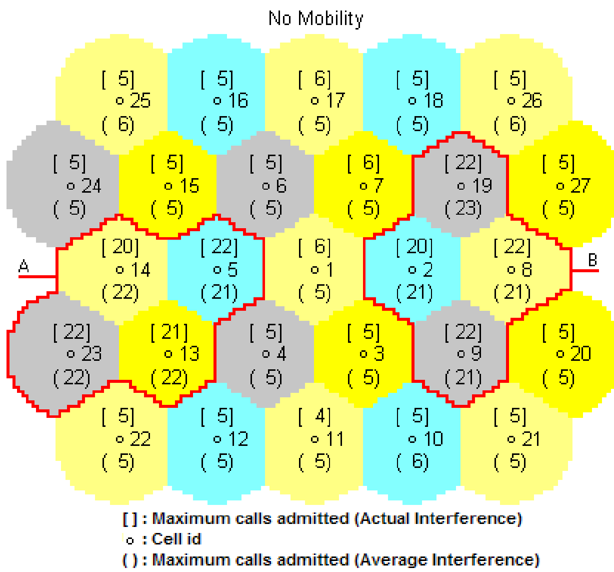

Figure 3.2: Maximum users admitted per cell for average and actual interference for no mobility case.

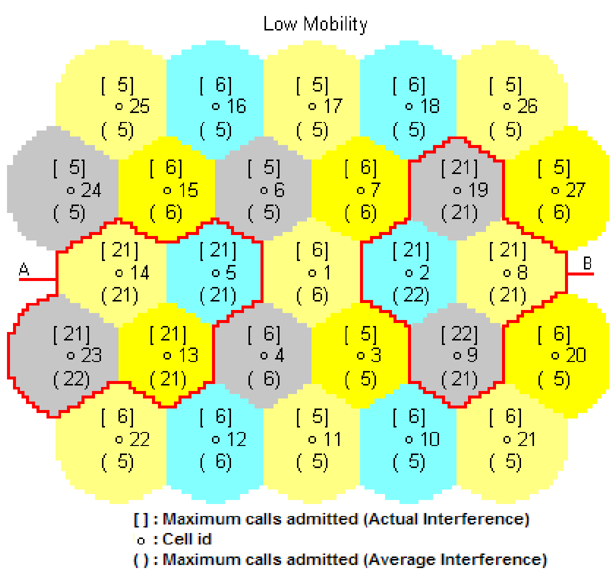

Figure 3.3: Maximum users admitted per cell for average and actual interference for low mobility case.

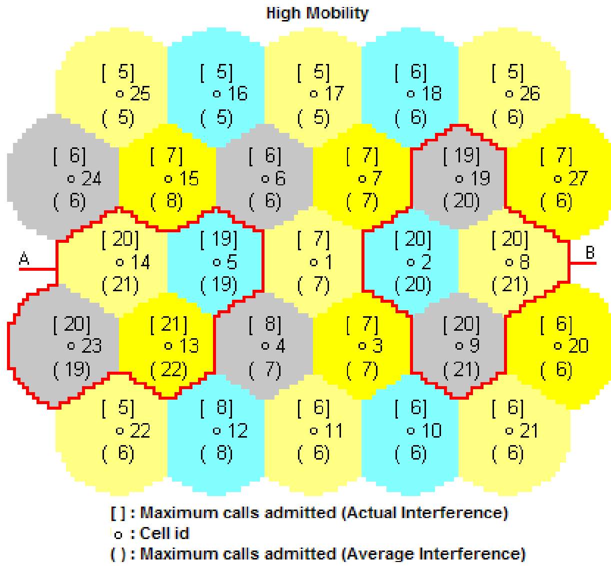

Figure 3.4: Maximum users admitted per cell for average and actual interference for high mobility case.

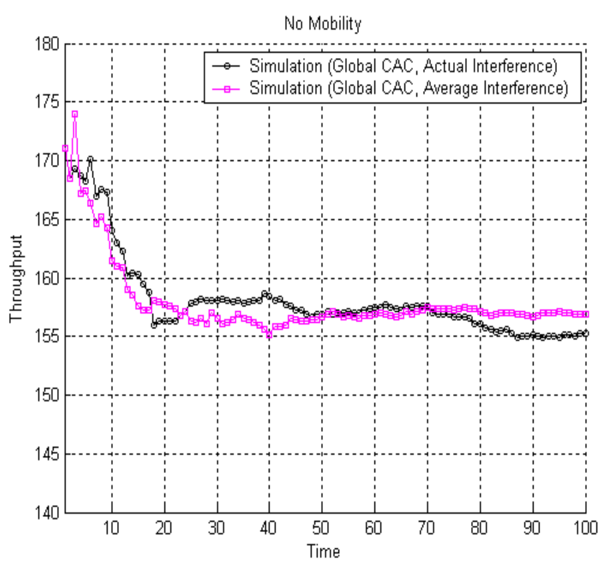

Figure 3.5: Network throughput for average and actual interference for no mobility case.

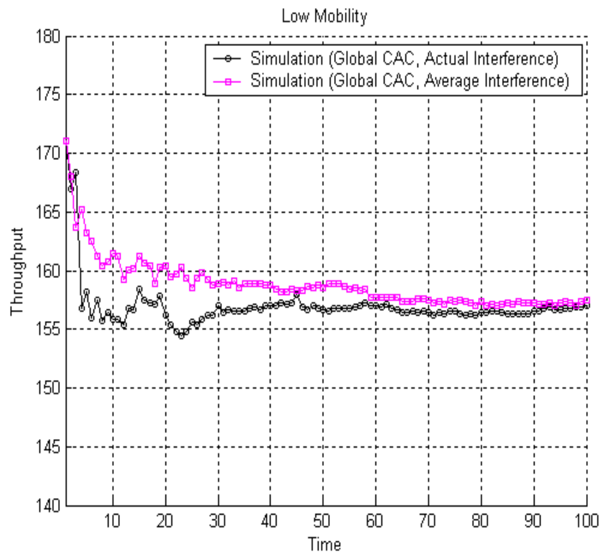

Figure 3.6: Network throughput for average and actual interference for low mobility case.

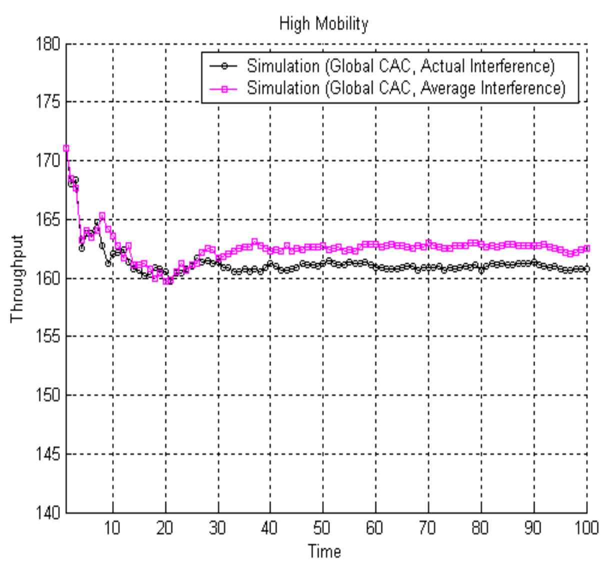

Figure 3.7: Network throughput for average and actual interference for high mobility case.

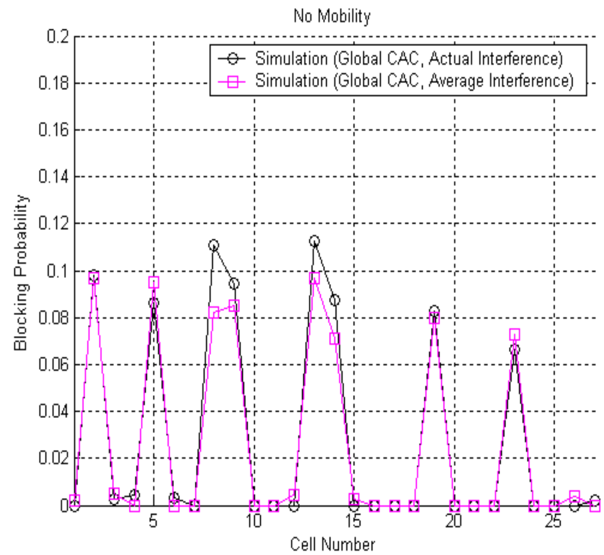

Figure 3.8: Blocking probability in every cell for average and actual interference for no mobility case.

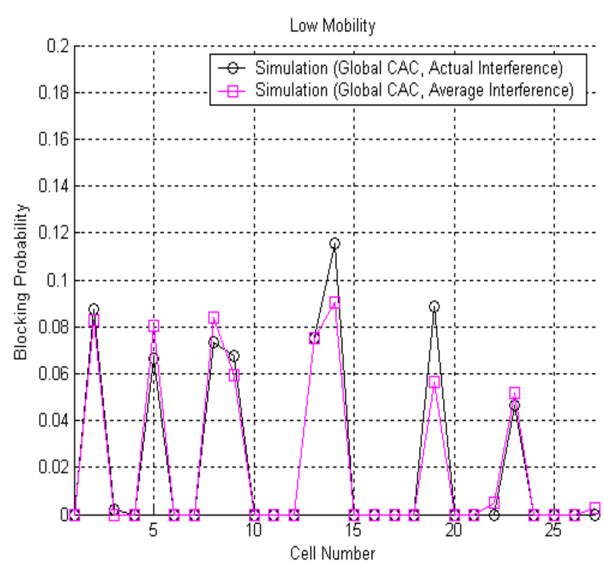

Figure 3.9: Blocking probability in every cell for average and actual interference for low mobility case.

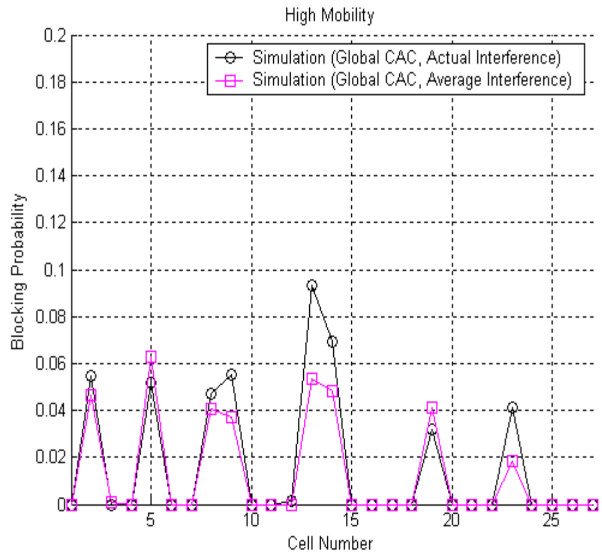

Figure 3.10: Blocking probability in every cell for average and actual interference for high mobility case.

actual interference. The range of calls for Group A and B varies from 19 to 23, and for the remaining cells from 4 to 8.

Figures 3.5, 3.6, and 3.7 show the throughput obtained using actual interference and average interference for the three mobility cases. Although the difference seen is not significant, the network throughput for average interference is a little higher than the network throughput for actual interference in all three cases. The throughput is highest for the high mobility case because the high mobility starts to equalize the non-uniform traffic distribution thus lowering the blocking probabilities, which leads to a gain in throughput.

The blocking probabilities for the three mobility cases are shown in Figures 3.8, 3.9, and 3.10. The maximum blocking probability for a cell in all three cases is nearly 0.1, which means that 1 call in every 10 calls is blocked. The blocking probabilities for average interference are lower than the blocking probabilities for actual interference for all three mobility cases but they are fairly close. Recall that the actual per user interference can be higher or lower than the average per user interference based on the user's actual location. In our simulations, even though the users were placed uniformly in a cell, the sum of the actual interference ended up being slightly higher than the average interference caused by the same number of users. This led to slightly higher blocking probabilities and thus slightly lower throughput.

3.8 Summary

We design and implement a global call admission control algorithm for a non-uniform traffic distribution. We use both relative average interference and relative actual interference. The algorithm also accounts for the mobility of users between cells. The requirement to maintain knowledge of the global state of the network makes the scaling exponential and henceforth computationally expensive. We simulate the network for varying mobility cases and show that the difference between the results obtained using average and actual interference is too small to justify the use of actual distance for determining interference.

CHAPTER 4

LOCAL CALL ADMISSION CONTROL

4.1 Introduction

Since the quality of a call in a CDMA network is affected by every other call present in the network, global CAC algorithms offer the most precise control over call admission policy. But such algorithms, even though optimal, carry sheer amount of computation complexity and are not easily scalable.

A simplified approach is to assume uniform traffic distribution with an equal number of simultaneous calls in every cell. This approach determines the maximum number of calls N per cell that can be allowed while maintaining required signal-to-interference ratio. This CAC algorithm is similar to fixed channel allocation system [26]. It would simply reject all the new calls when the upper limit N is exceeded. However, this approach is very inefficient for a CDMA network, since more calls can be admitted in a cell whose neighboring cells are thinly populated.

Assuming a uniform traffic distribution simplifies design but sacrifices performance. On the other hand, designing an optimal CAC algorithm, which minimizes the blocking probabilities for an arbitrary traffic distribution results in a design computational complexity which is exponential in the number of cells [9].

In this chapter, we formulate and simulate an optimized local CAC algorithm taking mobility and the traffic distribution into account. We study the performance of this CAC algorithm, and compare its network throughput to a traditional CAC algorithm where the maximum number of calls admitted is the same in every cell.

4.2 Local Call Admission Control Algorithm

The effectiveness of a CAC algorithm may be measured in terms of a network's throughput. In [3], the authors have formulated network throughput as

$$H = \sum_{i=1}^{M} \left\{ \lambda_i (1 - B_i) - B_i (\rho_i - \lambda_i) \right\}. \tag{4.1}$$

Thus a constrained optimization problem is formed in order to maximize network throughput with lower bounds on the signal-to-interference constraints in (2.7). The goal is to provide consistent grade of service while maintaining quality of service for a given traffic distribution profile. The optimization problem for the traditional CAC algorithm is given by

$$\begin{aligned} \max_{(N_1,\ldots,N_M)} \quad & H, \\ \text{subject to} \quad & N_i + \sum_{j=1}^{M} N_j F\left[j,i\right] \leq \; c_{eff}, \\ & \text{for} \quad i = 1, ..., M, \end{aligned} \tag{4.2}$$

where the solution to (4.2) provides the CAC algorithm with the values of $(N_1, ..., N_M)$, the maximum number of calls that can be admitted in each cell in the network.

For comparison, a traditional CAC algorithm is also formulated where the maximum number of calls, N, allowed in every cell is equal for all the cells in the network. The optimization problem is given by

$$\begin{aligned} \max_{(N)} \quad & H, \\ \text{subject to} \quad & N + \sum_{j=1}^{M} N F\left[j,i\right] \leq \; c_{eff}, \\ & \text{for} \quad i = 1, ..., M. \end{aligned} \tag{4.3}$$

Maximizing the throughput results in the largest possible N that meets the signal-to-interference constraints, and as a consequence results in the smallest possible blocking probabilities for all the cells.

4.3 Simulator Model

The functional flow and modular structure of our local CAC algorithm simulator is shown in Fig. 4.1.

4.3.1 Call Arrival and Admission Module

The simulator initiates by taking λ_i, a set of mean arrival rates, and N_i, a set of maximum number of calls allowed for every cell, as input to the call arrival module. The module calculates total offered traffic $\rho_i(t)$ using (3.5) and passes control to the call admission module.

The call admission module for our local CAC algorithm is much simpler to implement than our global CAC algorithm. Since N_i is known in advance (as a result of the optimization (4.2)) there is no need to calculate the inter-cell interference of each call. Thus the number of new calls that can be admitted, $A_i(t)$, for the present time unit is determined immediately.

4.3.2 Call Removal Module

The call removal module for our local CAC algorithm is exactly same as the call removal module of our global CAC simulator model.

4.4 Numerical Results

The network configuration, parameters, and mobility scenarios are the same as described in Chapter 3. Figures 4.2, 4.3, and 4.4 show Erlang traffic per cell, which is the sum of the new call arrival rates and the handoff calls, divided by the departure rates, in square brackets. The Figures also show that maximum number of calls that can be admitted in a cell in parenthesis as a result of the optimization in (4.2) for all three mobility cases. For the traditional CAC algorithm, for the same arrival rates and network parameters, the

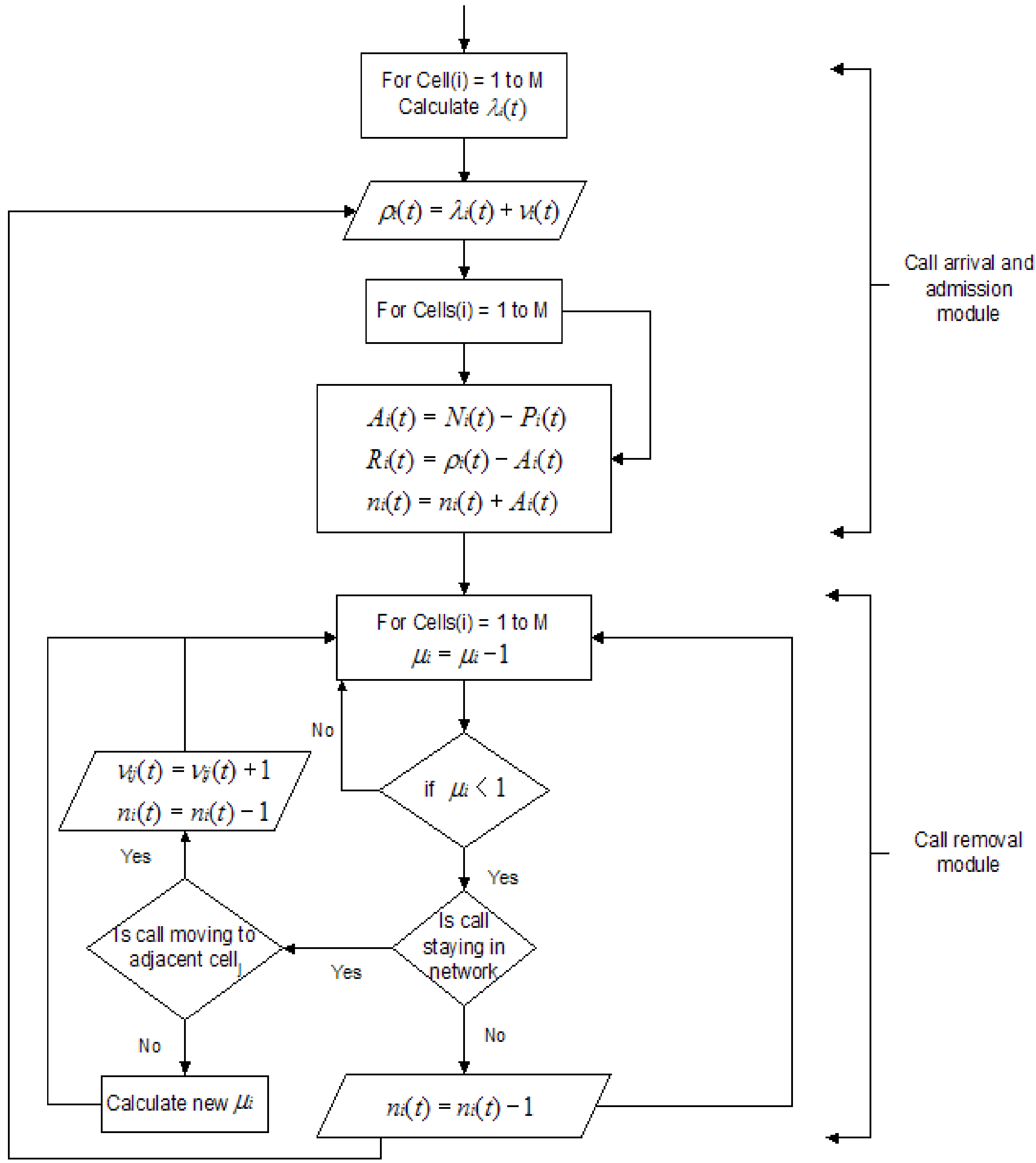

Figure 4.1: Flowchart of the network simulator model for our local CAC algorithm.

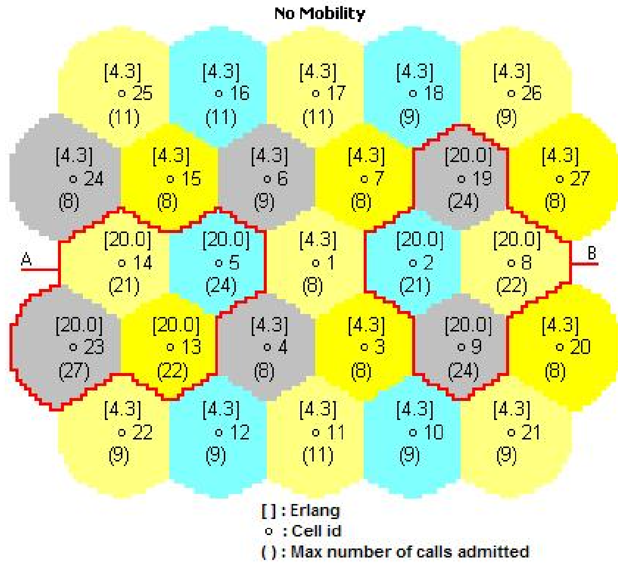

Figure 4.2: Erlang traffic and maximum number of calls allowed to be admitted per cell for a network with no mobility of users.

optimization (4.3) yields 18 users per cell, which is the upper bound on the maximum calls that can be admitted in every cell irrespective of the actual traffic in each cell.

Our optimized CAC algorithm adapts the maximum number of calls that can be admitted in each cell in response to the changes in traffic demand due to user mobility. It can been seen from Figures 4.2, 4.3, and 4.4 that the algorithm results in varying N_i's for every cell for all cases unlike the traditional CAC. Erlang traffic is also not the same for the three mobility cases. As the mobility increase, the Erlang traffic for cells in Group A and B decreases, and for some of the remaining cells, it increases. For example, in cell 5, the Erlang traffic decreases gradually from 20.0 to 17.0 as the mobility increases, but for cell 1, the Erlang traffic increases from 4.3 to 5.2. However, the total Erlang traffic for the entire network is constant for all the mobility cases.

Figures 4.5, 4.6, and 4.7 show the theoretical and simulated throughput for our optimized CAC algorithm for no, low, and high mobility, respectively. It can be seen that the simulated throughput is quite close to the theoretical throughput for all three mobility cases. The maximum difference between the theoretical throughput and the throughput obtained from

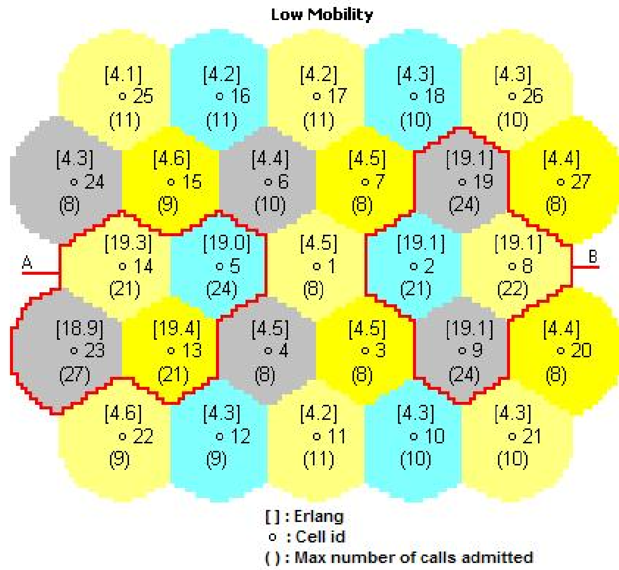

Figure 4.3: Erlang traffic and maximum number of calls allowed to be admitted per cell for a network with low mobility of users.

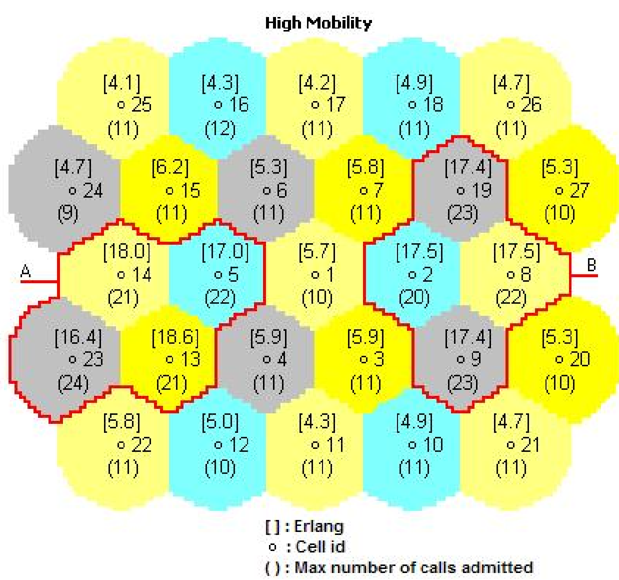

Figure 4.4: Erlang traffic and maximum number of calls allowed to be admitted per cell for a network with high mobility of users.

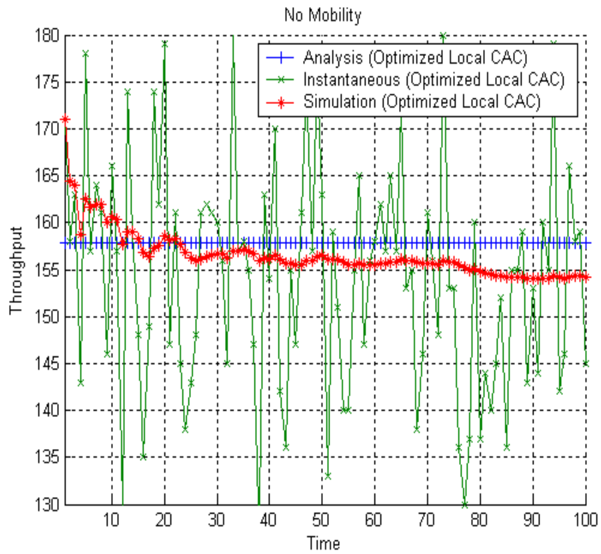

Figure 4.5: Network throughput for optimized local CAC for no mobility case.

simulation is less than 3.5%. Also, the throughput obtained from simulation is always lower than the throughput obtained theoretically. The difference is attributed to round off errors, since the number of arriving calls is rounded to the closest lower integer value.

Theoretical and simulated throughput for the traditional CAC algorithm are plotted against our optimized CAC algorithm, as shown in Figures 4.8, 4.9, and 4.10. Clearly, the optimized CAC algorithm is outperforming the traditional CAC algorithm in both simulation and theoretical throughput by a difference of 10% to 13% for all the three mobility cases.

The blocking probabilities obtained theoretically and from simulations are almost identical as seen in Figures 4.11, 4.12, 4.11, for both, optimized and traditional CAC algorithms. The traditional CAC algorithm has almost zero blocking probability for the cells with low traffic, and very high blocking probability for the cells with high traffic. On the other hand, the optimized CAC algorithm strikes a good balance between the blocking probabilities of the low and high traffic cells, and thus provides better grade of service.

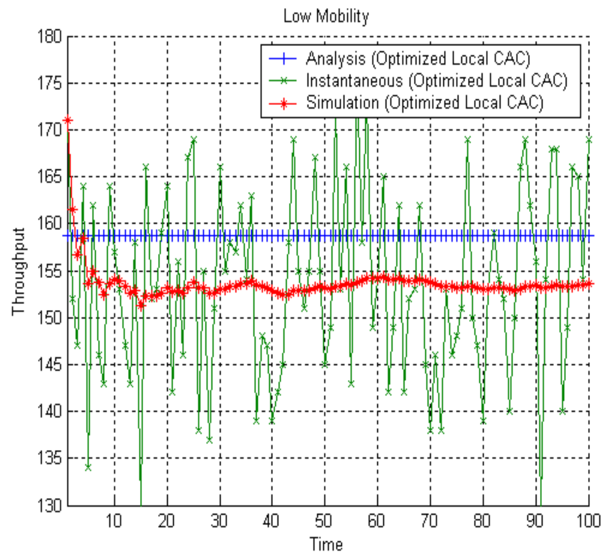

Figure 4.6: Network throughput for optimized local CAC for low mobility case.

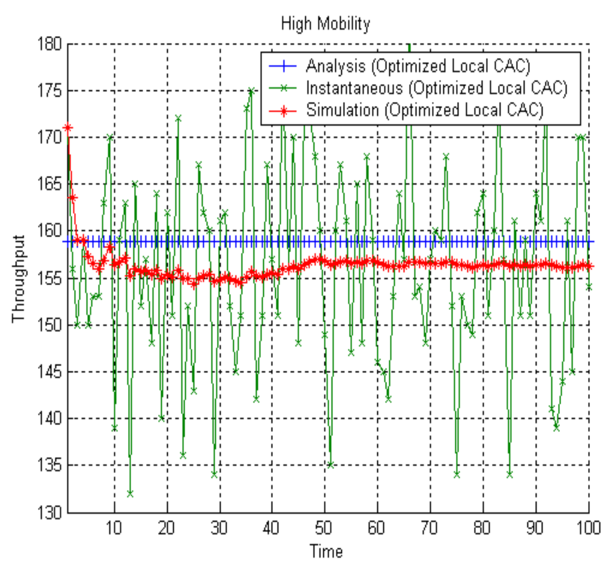

Figure 4.7: Network throughput for optimized local CAC for high mobility case.

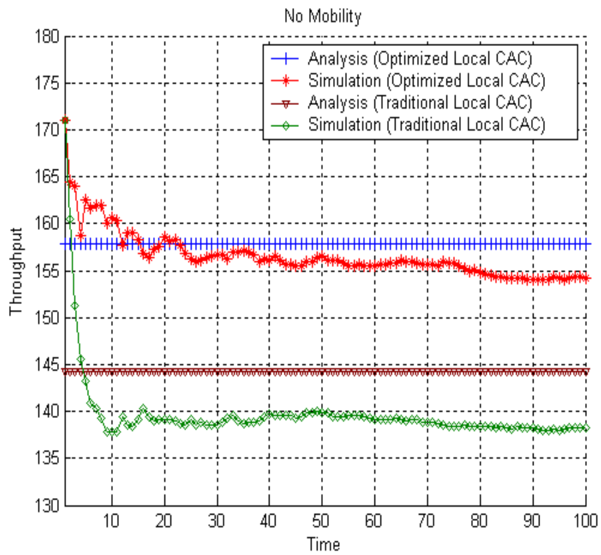

Figure 4.8: Theoretical and simulated network throughput for our local CAC and traditional local CAC for no mobility case.

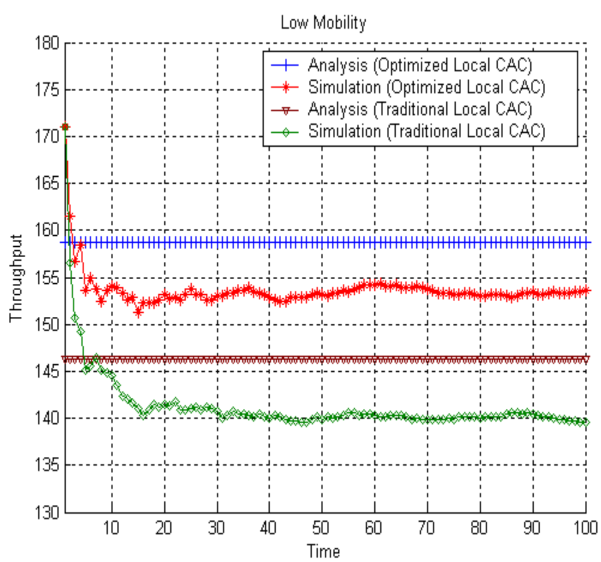

Figure 4.9: Theoretical and simulated network throughput for our local CAC and traditional local CAC for low mobility case.

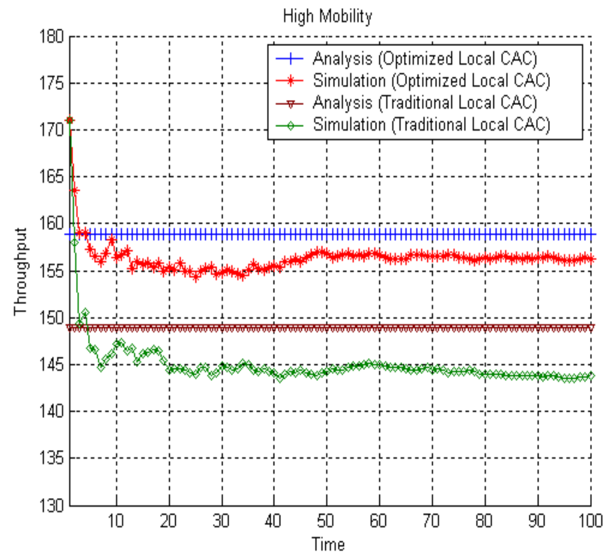

Figure 4.10: Theoretical and simulated network throughput for our local CAC and traditional local CAC for high mobility case.

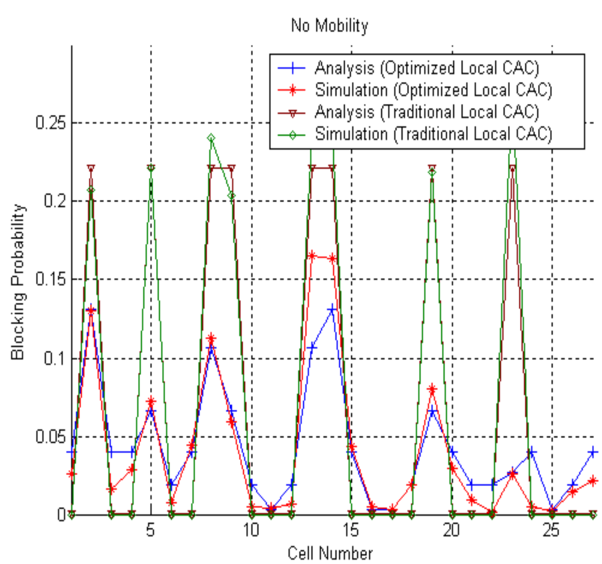

Figure 4.11: Theoretical and simulated blocking probabilities for our local CAC and traditional local CAC for no mobility case.

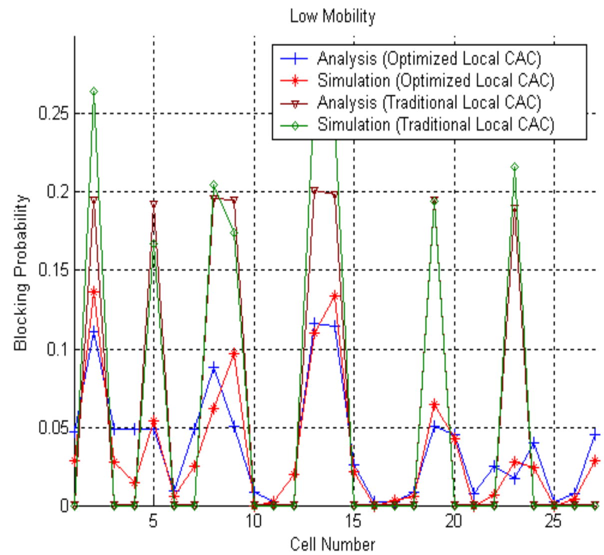

Figure 4.12: Theoretical and simulated blocking probabilities for our local CAC and traditional local CAC for low mobility case.

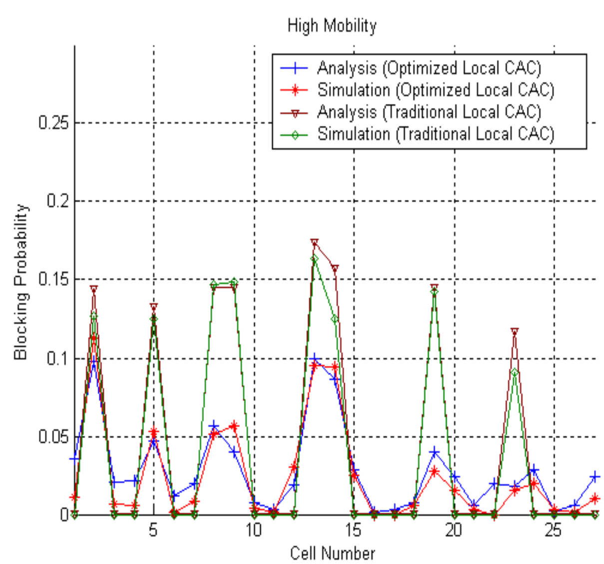

Figure 4.13: Theoretical and simulated blocking probabilities for our local CAC and traditional local CAC for high mobility case.

4.5 Summary

We design and simulate an optimized local CAC algorithm that scales linearly in the number of the cells, and accounts for the mobility of users and the traffic distribution profile. The algorithm is based on the formulation of an optimization problem that maximizes the network throughput using SIR as the lower bound. We compare the performance of our optimized local CAC algorithm in terms of blocking probabilities and network throughput to a traditional CAC algorithm. For a uniform traffic distribution, the performance is almost identical, but for non-uniform traffic distribution, our local CAC algorithm outperforms the traditional CAC algorithm.

CHAPTER 5

GLOBAL CAC VERSUS LOCAL CAC

5.1 Introduction

Call admission control algorithms are used to decide whether or not a network should accept a new call. A CAC algorithm is considered global if the decision to admit a call is based on the current total number of calls in the network, and local if the algorithm considers only a single cell for making that decision. However, their design may look at the network as a whole. A global CAC is a centralized scheme while a local CAC is distributed in nature. Each approach has advantages and disadvantages. In this chapter, we compare both models in terms of complexity, implementation, and performance.

5.2 CAC Comparison

One objective of a CAC algorithm is to admit as many calls as possible without degrading the quality of calls already present in the network. Our CAC algorithms, global as well as local, preserve the quality of service offered by the network by maintaining a user configuration which always satisfies the set of equations given by (2.7). It is the time when this configuration is computed that sets our global CAC algorithm apart from our local CAC algorithm.

For every new arriving call, our global CAC algorithm dynamically determines if the call should be admitted by solving (2.7) in real time. On the other hand, our local CAC algorithm, for a given traffic distribution profile, obtains an optimized set of users for every cell by solving the constraint problem given by (4.2) in advance. Consequently our local CAC algorithm has determined the maximum number of users that can be admitted in every cell beforehand. Thus, our local CAC algorithm avoids the real time interference calculation overhead by shifting the calculation complexity to solving the optimization problem offline.

As a result, though our local CAC algorithm is much faster in execution than our global CAC algorithm, it can only compensate for large fluctuation in traffic distribution by resolving the optimization problem. While our global CAC algorithm is inherently optimized and can adapt to varying traffic distribution, our local CAC algorithm is optimized only for a given set of traffic distribution. In other words, our local CAC algorithm performance will deteriorate if the actual traffic distribution is different from the traffic profile that is used during optimization.

5.3 Simulator Model Comparison

Our simulator models for the global and local CAC algorithms (shown in Figures 3.1 and 4.1, respectively,) are identical in order of execution of modules but differ in implementation of the call admission control. Our local CAC algorithm performs the time consuming optimization in advance and calculates the solution, which is the set of maximum calls admissible for every cell before starting the simulation. Thus, these offline calculations not only obviate the necessity to calculate the inter-cell interference for every new call but also make it possible for the call admission module to know the number of calls that it can allow in a cell in a single execution loop.

The call admission control is much more complex for our global CAC algorithm since it performs real time calculations of inter-cell interference for every arriving call to determine if the call can be admitted. Thus, the call admission control has a computational complexity that is $O({c_{eff}}^M)$ compared to $O(M)$ for our local CAC algorithm. Consequently, our local CAC algorithm simulator is much faster than our global CAC algorithm simulator.

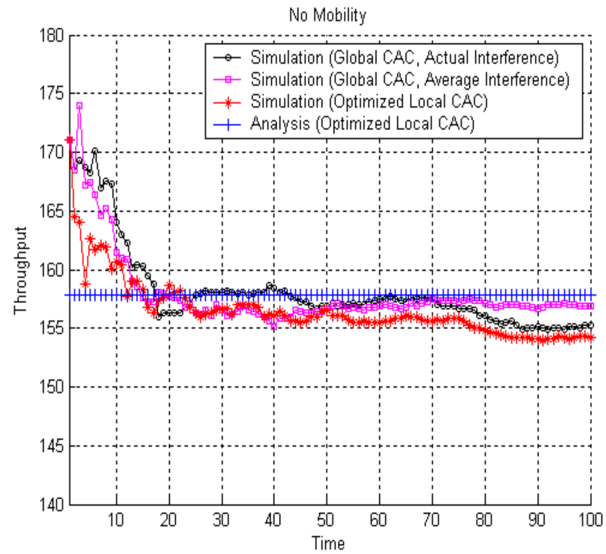

Figure 5.1: Network throughput for our optimized local CAC and global CAC algorithms for no mobility case.

5.4 Numerical Results

Our global CAC algorithm is inherently optimized, and therefore it is expected to perform better than our local CAC algorithm. It is shown from Figures 5.1, 5.2, and 5.3, for no, low, and high mobility cases, respectively, that indeed our global CAC algorithm throughput is always a little higher than our local CAC algorithm. However, the difference between our global CAC throughput and our local CAC throughput is between 1% and 3% for all the three mobility cases . In accordance with the conclusions drawn from throughput results, the blocking probabilities for our global CAC algorithm are marginally lower than our local CAC algorithm for all the three mobility cases as seen in Figures 5.4, 5.5, and 5.6.

5.5 Summary

We compare our global CAC algorithm and local CAC algorithm in terms of computational complexity, simulation model, and performance. Our global CAC algorithm has a computational complexity of $O({c_{eff}}^M)$ while our optimized local CAC has a computational

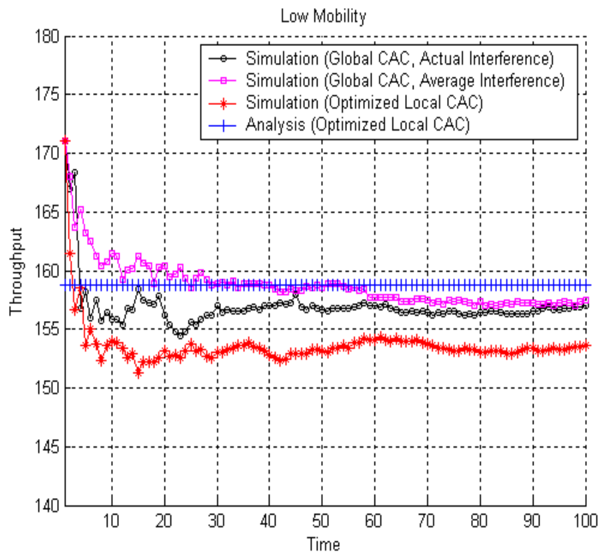

Figure 5.2: Network throughput for our optimized local CAC and global CAC algorithms for low mobility case.

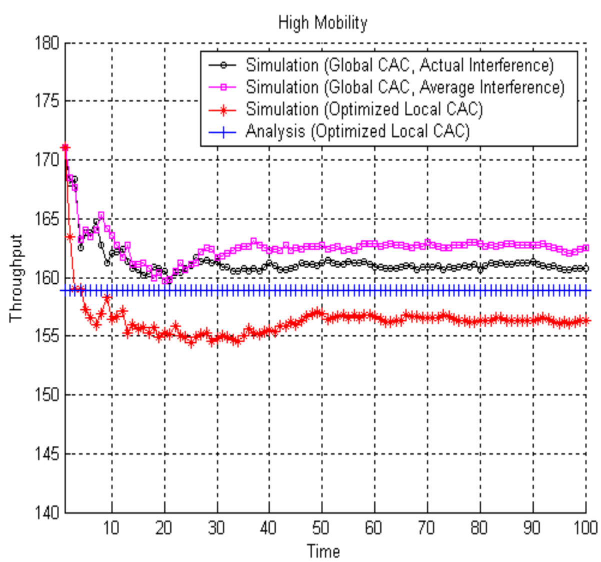

Figure 5.3: Network throughput for our optimized local CAC and global CAC algorithms for high mobility case.

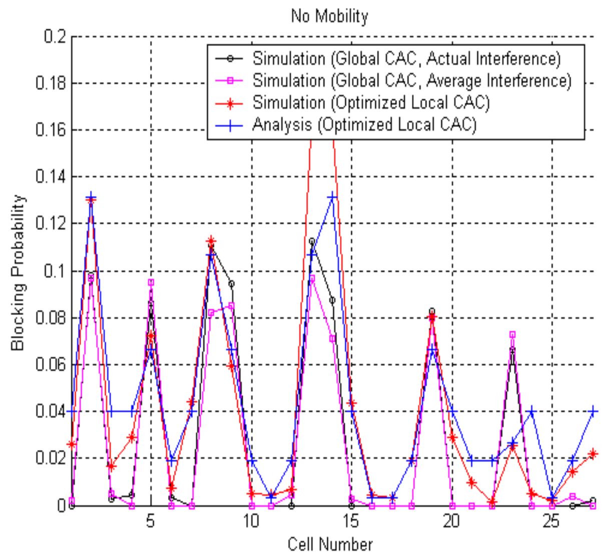

Figure 5.4: Blocking probability for our optimized local CAC and global CAC algorithms for no mobility case.

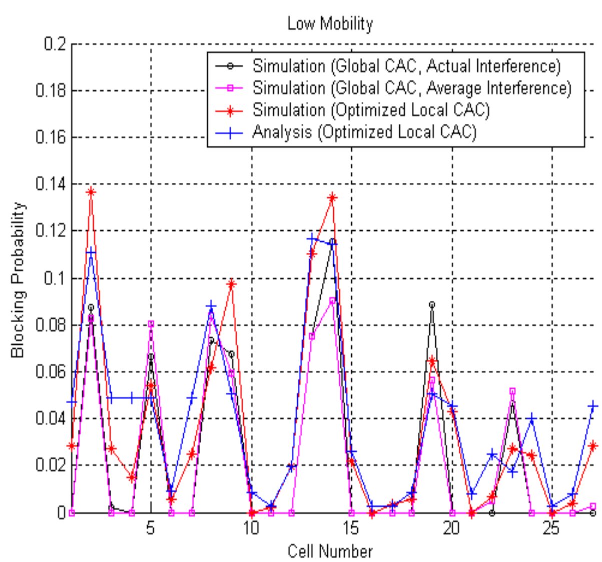

Figure 5.5: Blocking probability for our optimized local CAC and global CAC algorithms for low mobility case.

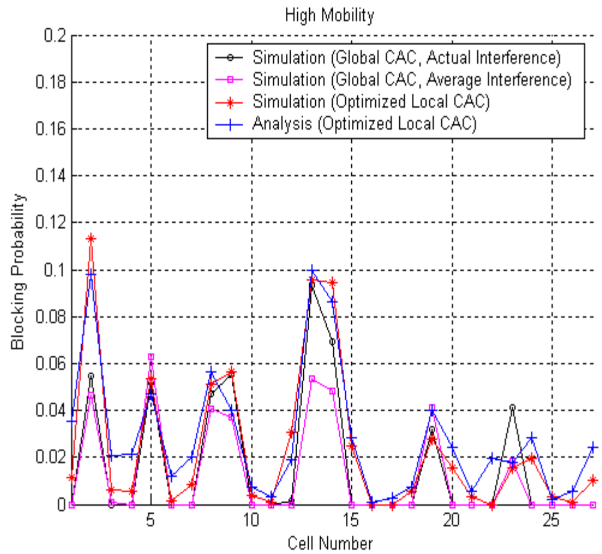

Figure 5.6: Blocking probability for our optimized local CAC and global CAC algorithms for high mobility case.

complexity of $O(M)$. Our simulation results show that the difference between our optimized local CAC algorithm's performance and our global CAC algorithm's performance is small enough (less than 3%) to justify the small tradeoff low throughput for the huge reduction in computational complexity.

CHAPTER 6

CONCLUSIONS

6.1 Summary

CDMA is an interference limited multiple access technology. Because all users share the entire available bandwidth, self interference generated by the users is the most significant factor in determining network capacity. A large number of models in the literature use average interference for the calculation of capacity and designing call admission control algorithms. The advantage gained in reduction in computational complexity by using such models comes at the cost of rendering the exact location of a user within a cell irrelevant.

In Chapter 2, we design average and actual relative per-user inter-cell interference models and analyze the effect of user-distribution on the capacity of a twenty-seven cell CDMA network through simulations.

In average inter-cell interference models, the interference caused by a user in a cell is represented by the average interference offered by that cell, which is computed by averaging the interference over that cell area. Our actual inter-cell interference model uses actual distance of users from base stations to compute exact interference. We calculate the theoretical network capacity by formulating and solving a constrained optimization problem. Then through simulations, we show that the capacity obtained using average interference is a good approximation to the capacity calculated using actual interference for a uniform user distribution. However, for a non-uniform user distribution, the capacity obtained using actual interference may exceed or diminish the capacity obtained using average interference by large margins.

In Chapter 3, we design and implement a global call admission control algorithm for arbitrary traffic distribution using the actual and average inter-cell interference models we developed in Chapter 2. The algorithm also takes users mobility between cells into account.

We analyze the effects of using average versus actual interference in terms of blocking probabilities and network throughput through simulations for varying mobility cases. Our results show that the network throughput obtained using average interference is slightly more than the throughput obtained using actual interference. Furthermore, the network throughput for high mobility is highest among the three mobility cases. The high mobility equalizes the non-uniform traffic distribution thus lowering the blocking probabilities, which leads to a gain in throughput.

In Chapter 4, we design and simulate a local CAC algorithm by formulating an optimization problem that maximizes the network throughput using the signal-to-interference constraints as lower bounds. The solution to this problem is the maximum number of users that can be admitted in every cell. Thus, even though our local CAC algorithm implementation is simple and considers only a single cell for admitting a user, its design is optimized for the entire network and a given traffic distribution profile.

We compare the performance of our optimized local CAC algorithm in terms of blocking probabilities and network throughput to a traditional CAC algorithm where the maximum number of users allowed in each cell is the same. Our simulation results show that for a uniform traffic distribution, the performance is almost identical, but for non-uniform traffic distribution, our network throughput is consistently higher than the traditional CAC algorithm's throughput for all mobility cases.

Finally, in Chapter 5, we compare our global and local CAC algorithms in terms of computational complexity, simulation model, and performance. Our global CAC algorithm, even though inherently optimized for any traffic distribution profile, bears the overhead of real time interference calculations for every arriving call. On the other hand, our local CAC algorithm performs its time consuming optimization calculations in advance and uses the solution obtained for call admission control. Consequently, our local CAC is simpler to implement, and is much faster to execute. The simulation results show that the optimized local CAC achieves almost the same performance as our global CAC in terms of blocking probabilities and network throughput for a given traffic distribution profile.

6.2 Future Research

We conclude by outlining possible directions for future research:

- The algorithm can be further extended to include prioritization of handoff calls over new calls by resource pooling. It may be achieved by maintaining two different signal-to-interference threshold.

- WCDMA and CDMA 2000 are 3G evolutions of present 2G CDMA systems. These technologies deliver higher and multiple data rates. The optimization techniques discussed in this work can take advantage of the multi-rate transmission ability of the 3G systems. The simulator can be extended to include the characteristics of these technologies.

BIBLIOGRAPHY

[1] R.G. Akl, M.V. Hegde, A. Chandra, and P.S. Min. CCAP: CDMA Capacity Allocation and Planning. Technical report, Washington University, April 1998.

[2] R.G. Akl, M.V. Hegde, M. Naraghi-Pour, and P.S. Min. Multi-cell CDMA network design. *IEEE Transactions on Vehicular Technology*, 50(3):711–722, May 2001.

[3] R.G. Akl, M.V. Hegde, M. Naraghi-Pour, and P.S. Min. Call admission control scheme for arbitrary traffic distribution in CDMA cellular systems. *IEEE Wireless Communications and Networking Conference*, pages 465–470, September 2000.

[4] S. Anand, A. Chockalingam, and K. N. Sivarajan. Outage and capacity analysis of cellular CDMA with admission control. *IEEE Wireless Communications and Networking Conference*, 2:908–912, March 2002.

[5] A. Baiocchi, F. Sestini, and F. Priscoli. Effects of user mobility on the capacity of a CDMA network. *European Transactions on Telecommunications*, 7(4):305–314, July-August 1996.

[6] M.S. Bazaraa and J.J. Jarvis. *Linear Programming and Network Flows.* John Wiley & Sons, 1977.

[7] T. Dohi, M. Sawahashi, and F. Adachi. Performance of SIR based power control in the presence of non-uniform traffic distribution. *IEEE International Conference on Universal Personal Communications*, pages 334–338, November 1995.

[8] J.S. Evans and D. Everitt. On the teletraffic capacity of CDMA cellular networks. *IEEE Transactions on Vehicular Technology*, 48(1):153–165, January 1999.

[9] D. Everitt. Analytic traffic models of CDMA cellular networks. *Proceedings of the 14th International Teletraffic Congress*, pages 349–356, June 1994.

[10] G.J. Foschini, B. Gopinath, and Z. Miljanic. Channel cost of mobility. *IEEE Transactions on Vehicular Technology*, 42(4):414–424, November 1993.

[11] G.J. Foschini and Z. Miljanic. A simple distributed autonomous power control algorithm and its convergence. *IEEE Transactions on Vehicular Technology*, 42(4):641–646, November 1993.

[12] K.S. Gilhousen, I.M. Jacobs, R. Padovani, A.J. Viterbi, L.A. Weaver, and C.E. Wheatley. On the capacity of a cellular CDMA system. *IEEE Transactions on Vehicular Technology*, 40(2):303–312, May 1991.

[13] S. Glisic and B. Vucetic. *Spread Spectrum CDMA Systems for Wireless Communications*. Artech House, 1997.

[14] S.V. Hanly. Capacity and power control in spread spectrum macrodiversity radio networks. *IEEE Transactions on Communications*, 44(2):247–256, February 1996.

[15] S.V. Hanly. An algorithm for combined cell-site selection and power control to maximize cellular spread spectrum capacity. *IEEE Journal on Selected Areas in Communications*, 13(7):1332–1340, September 1995.

[16] Y. Ishikawa and N. Umeda. Capacity design and performance of call admission control in cellular CDMA systems. *IEEE Journal on Selected Areas in Communications*, 15(8):1627–1635, October 1997.

[17] Joonhwan Kim, Young-June Choi, and Saewoong Bahk. Interference-based capacity analysis in CDMA cellular systems. *IEEE Wireless Communications and Networking Conference*, 2:1412–1417, March 2003.

[18] Kyoung II Kim. CDMA cellular engineering issues. *IEEE Vehicular Technology Conference*, 42:345–350, Aug. 1993.

[19] D. Lam, D.C. Cox, and J. Widom. Traffic modeling for personal communication services. *IEEE Communications Magazine*, pages 79–87, February 1997.

[20] K.K. Leung, W.A. Massey, and W. Whitt. Traffic models for wireless communication networks. *IEEE Journal on Selected Areas in Communications*, 12(8):1353–1364, October 1994.

[21] J.G. Markoulidakis, G.L. Lyberopoulos, D.F. Tsirkas, and E.D. Sykas. Mobility modeling in third-generation mobile telecommunications systems. *IEEE Personal Communications*, pages 41–56, August 1997.

[22] David W. Matolak and Anjula Thakur. Outside cell interference dynamics in cellular CDMA. *Proceedings of the 35th Southeastern Symposium*, pages 418–152, March 2003.

[23] K. Nakano, K. Saita, N. Karasawa, M. Sengoku, and S. Shinoda. Teletraffic characteristics in cellular systems and traffic flow in road systems. *IEEE Vehicular Technology Conference*, 1999.

[24] P.V. Orlik and S.S. Rappaport. A model for teletraffic performance and channel holding time characterization in wireless cellular communication with general session and dwell time distributions. *IEEE Journal on Selected Areas in Communications*, 16(5):788–803, June 1998.

[25] R. Padovani. Reverse link performance of IS-95 based cellular systems. *IEEE Personal Communications*, 1(3):28–34, Third Quarter 1994.

[26] K.W. Ross. *Multiservice Loss Models for Broadband Telecommunication Networks.* Springer, 1995.

[27] C.U. Saraydar and A. Yener. Capacity enhancement for CDMA systems through adaptive cell sectorization. *IEEE Wireless Communications and Networking Conference*, pages 1139–1143, September 1999.

[28] S. Seo, T. Dohi, and F. Adachi. SIR-Based transmit power control of reverse link for coherent DS-CDMA mobile radio. *IEICE Transactions on Communications*, E81-B(7):1508–1516, July 1998.

[29] S. Shin, C. Cho, and D. Sung. Interference-based channel assignment for DS-CDMA cellular systems. *IEEE Transactions on Vehicular Technology*, 48(1):233–239, January 1999.

[30] M. Soleimanipour and G.H. Freeman. A realistic approach to the capacity of cellular CDMA systems. *IEEE Vehicular Technology Conference*, 2:1125–1129, 1996.

[31] K. Takeo and S. Sato. Evaluation of a CDMA cell design algorithm considering non-uniformity of traffic and base station locations. *IEICE Transactions Fundamentals*, E81-A(7):1367–1377, July 1998.

[32] K. Takeo and S. Sato. The proposal of CDMA cell design scheme considering change in traffic distributions. *IEEE International Symposium on Spread Spectrum Techniques and Applications*, 1:229–233, September 1998.

[33] Y. Takeuchi. Results of multiple cell simulations of a CDMA cellular system focusing on SIR based power control. *IEEE International Conference on Communications*, 1:63–67, June 1998.

[34] C. Tellez-Labao, J.M. Romero-Jerez, and A. Diaz-Estrella. Capacity analysis of SIR-based power-controlled CDMA systems under multipath fading. *Personal, Indoor and Mobile Radio Communications*, 3:1237 –1241, Sept. 2002.

[35] A.J. Viterbi. *CDMA Principles of Spread Spectrum Communication.* Addison-Wesley, 1995.

[36] A.J. Viterbi, A.M. Viterbi, K.S. Gilhousen, and E. Zehavi. Soft handoff extends CDMA cell coverage and increases reverse link capacity. *IEEE Journal on Selected Areas in Communications*, 12(8):1281–1288, October 1994.

[37] A.M. Viterbi and A.J.Viterbi. Erlang capacity of a power controlled CDMA system. *IEEE Journal on Selected Areas in Communications*, 11(6):892–900, August 1993.

[38] P.E. Wirth. The role of teletraffic modeling in the new communications paradigms. *IEEE Communications Magazine*, pages 86–92, August 1997.

[39] J. Yang and W.C.Y. Lee. Design aspects and system evaluation of IS-95 based CDMA systems. *IEEE International Conference on Universal Personal Communications*, pages 381–385, October 1997.

[40] R.D. Yates. A framework for uplink power control in cellular radio systems. *IEEE Journal on Selected Areas in Communications*, 13(7):1341–1347, September 1995.

[41] M.M. Zonoozi and P. Dassanayake. User mobility modeling and characterization of mobility patterns. *IEEE Journal on Selected Areas in Communications*, 15(7):1239–1252, September 1997.